AIAA SciTech Forum
23-27 January 2023, National Harbor, MD & Online
AIAA SCITECH 2023 Forum

10.2514/6.2023-2262

Fabrication and Characterization of a Large-array Hot-film Sensor for Detection of Separated Flow

Sean Wang* and Mark A. Miller†
Penn State University, University Park, PA, 16802

Hot-film anemometers relate heat transfer on a small resistive element to local velocity and shear stress in a flow. Large-array surface-mounted hot-films expand velocity and stress measurements to an entire surface, enabling measurement of unsteady flow phenomena including separation. The development of these sensor arrays requires alternative methods of fabrication in addition to analysis of sensor frequency response and methods of data validation. Various applications exist where information on the boundary layer state is desired, such as a wind turbine blade, but due to the physically large scales a standard hot-film sensor remains impractical. This work centers on fabrication and testing of a large-scale, surface-mount, hot-film sensor array. The objective of the array is to provide information on the flow condition, specifically whether the flow remains attached or separated, under unsteady inflow conditions. A constant temperature anemometer (CTA) is used to resolve the flow condition under unsteady inflow, including detection of flow separation or unsteadiness due to turbulence. The sensor array response is verified using fluorescent oil film for the static case and particle image velocimetry for the dynamic velocity tests. The CTA demonstrates sensitivity to separated, attached, and turbulent boundary layer states through variance integration in the frequency domain. A simple classification system based on the measured variance is provided for flow state identification at the low Reynolds number (Re) which were tested.

I. Nomenclature

α	=	angle of attack
c	=	chord length
C_p	=	power coefficient
CTA	=	constant temperature anemometer
μ	=	dynamic viscosity
OHR	=	overheat ratio
PIV	=	particle image velocimetry
ρ	=	density
Re	=	Reynolds number
TRF	=	toner reactive foil
U	=	wind tunnel velocity
x/c	=	non-dimensional chord length

II. Introduction

A hot-film is a heat-transfer based flow sensor that can be used to quantify the local velocity or shear stress at a point of interest in a flow. In an array configuration, surface-mount hot-films can provide important information on the flow condition over an aerodynamic surface. A hot-film array enables velocity measurements at locations which are inaccessible with conventional instrumentation, such as on the compound curved airfoil surfaces near a wind turbine blade root, or over larger aircraft wing spans. Hot-film sensors have been used in a variety of applications such as the detection of transition [1], in morphing airfoil stall control[2], and to quantify boundary layer separation and reattachment[3], to name a few. Lee and Basu [4] provided detailed information on the boundary layer state using a

*Graduate Research Assistant, Aerospace Engineering, 229 Hammond Building, AIAA Member
†Assistant Professor, Aerospace Engineering, 230C Hammond Building, AIAA Member

closely-spaced hot-film array. They measured the array response under the influence of a dynamically changing angle attack, with the goal of that work being an exploration of dynamic stall phenomena. Few prior works have focused on evaluating lifting body response under dynamic inflow (varying velocity) which is more analogous to a gust or unsteady velocity event experienced in the atmospheric boundary layer.

Hot-film arrays present a variety of technical challenges over the single sensor element, including array assembly, electrical connection, substrate heat transfer, driving circuitry, and frequency response. A popular method of array fabrication is embedding the hot-film sensing element within a larger substrate [3, 5], however no prior works have yet addressed the challenge of scaling up an array to large sizes, on the order of several meters square, which would be appropriate for an application such as a wind turbine blade.

The effects of wind gusts play a large role in structural design and control systems for both horizontal and vertical axis wind turbines. The additional structural stresses incurred by from a rapid increase in wind speed have been shown to significantly alter the root section stresses of a model NREL Phase VI turbine [6] as well as result in torque oscillations in high solidity vertical axis turbines affecting the power coefficient C_p [7]. Studies regarding turbine gust response have so far have predominately been computational. A large hot-film array could be a principal validation point against existing computational studies as well as enable field measurement of the distribution and for the characterization of atmospheric gusts.

The current project is focused on the development of a large-scale hot-film array with a focus on making the array low-cost, scalable, and physically flexible so it can conform to large-scale, complex geometries. Before application in the field, the sensor array performance must be evaluated under known conditions. Key to this is an evaluation of the array flow separation detection capabilities as this will inform the final sensor application response to unsteady, gusting inflow conditions.

III. Experiment Setup

A. Hot-Film Array Fabrication

The large-array hot-film consists of two main parts, the hot-film sensors themselves and an etched copper substrate backing. The hot-film sensors chosen are commercially available, low-cost TaoSytems Senflex SF9902 sensors. These commercial sensors are pre-made and consist of a 0.1 mm wide by 1.45 mm long Nickel sensing element with a 6-8 Ω cold resistance and an approximate thickness of 50 µm. The substrates are etched from sheets of copper-clad polyimide film that have a combined thickness of 63.5 microns. The copper layer is etched to a depth such that the SF9902 sensors sit flush in the substrate. Preparation of the substrate consists of three main steps: layout design, masking, and etching.

Sensor substrate layouts are designed in Adobe Photoshop using the hot-film dimensions provided by the manufacturer. Key design elements for the substrate layout include drawing an appropriate area to act as the sensor beds, determining the number of sensors and orientation, and drawing leads and solder pads for external circuitry. After a satisfactory design is complete, the design is horizontally flipped in preparation to be used as a mask for the substrate.

The substrate mask is created using the dye transfer method. In the dye transfer method, the flipped substrate design is first printed onto a sheet of toner transfer paper. The design is then transferred onto the copper-clad polyimide by interfacing the toner side of the toner transfer paper with the copper side of the copper-clad polyimide and applying heat and pressure. A conventional laminator, in this case a Tamerica SM-330, can be used to transfer the design. After lamination the toner transfer paper and copper-clad polyimide must be rinsed with cold water for the toner to release and transfer properly. The result is a mask of the correctly-oriented substrate design on the copper-clad polyimide. The toner mask is still porous after dye transfer and needs to be sealed before etching. Toner reactive foil (TRF) is applied to the masked copper-clad polyimide using the laminator to create an impermeable mask, ready to be etched.

The TRF-sealed masked copper-clad polyimide is then etched by being submerged in ferric chloride. The etching process occurs over a series of chemical reactions and typically takes around 45 minutes for 63.5 µm thick copper-clad polyimide. Etching is complete when the translucent polyimide backing is plainly visible without any copper remaining. Once cleaned, the substrate is finished and is ready to be bonded with the hot-films to create the final array hot-film.

To bond the SF9902 hot-film sensors to the substrate, an adhesive is applied to the sensor bed, which fits an appropriately trimmed SF9902. Common commercial adhesives, such as 3M Super 77, are sufficient for adhering the hot-films to the substrate. Electrical continuity is achieved by soldering the substrate and hot-film sensor leads and creates the final array hot-film. Affixing the hot-film array to the aerodynamic surface of interest can also be done using 3M Super 77, with structural reinforcement with materials such as tape or stronger adhesives recommended in areas where concentrated cyclic loads are expected, such as areas where electrical leads connect the driving circuitry. The

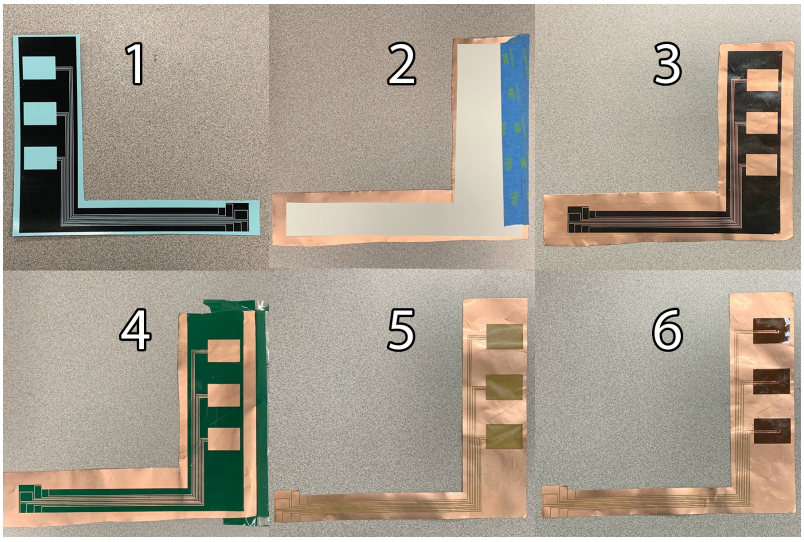

Fig. 1 The fabrication process for the array hot-film: steps 1, 2 show the dye transfer process, steps 3, 4 show the bare toner mask as well as the TRF-sealed mask, step 5, 6 show the etched copper substrate without and with the SF9902 sensors attached respectively.

combined hot-film and substrate designed for this study is a small-to-medium scale proof of concept as shown in figure 1. Full-scale versions of the hot-film array, which could be scaled up to 1 meter by 1 meter, would use a similar method of fabrication with modifications to the printing process and application of etchant to accommodate for the increased size.

B. Experimental Setup

The experimental setup consists of a linear array of three TaoSystems SF9902 surface mount hot-films used primarily for unsteady testing, as well as a single SF9902 used for static testing. Both configurations of combined hot-film and substrate(s) are adhered to an NACA 0012 airfoil with chord length, c, of approximately 14.22 cm. The linear hot-film array is oriented such that the sensing elements are aligned along the airfoil chord. The airfoil is mounted as close as possible to the wind tunnel outlet centerline in order to minimize turbulent flow and shear effects. A pitot-static tube is mounted near the centerline of the wind tunnel exit to measure wind speed and is connected to a Validyne pressure transducer. A type-K thermocouple is used to measure temperature. The qwiic system, a proprietary i^2c interface, is used to obtain temperature data, initially read into an Arduino which generates an output temperature signal read again by LabVIEW.

The hot-films were driven by a constant temperature anemometer (CTA) circuit. The CTA was a commercial unit from TSI (IFA-300) capable of driving two hot-film channels concurrently. The first and last hot-films in the array were driven simultaneously in experiments to better characterize sensor performance due to shifting of the separation location. Using the CTA, a conservative overheat ratio (OHR) of 0.45, was applied to both hot-films. A low-cost CTA circuit is being developed for future use in driving a larger sensor array.

An open jet wind tunnel was used to test the hot-film array under both steady and unsteady inflow conditions to elicit information about the sensor separation detection capabilities and frequency response. The open jet wind tunnel consists of an axial air blower, a diffuser housing with multiple screens, a plenum chamber, a high area ratio circular nozzle, and a circular to square transition nozzle with outlet dimensions 8 inches by 8 inches. The wind tunnel is shown schematically in figure 2. The test section velocity is continuously adjustable via a Dynamatic AF 1500 AC motor controller connected to the wind tunnel blower. The wind tunnel can produce velocities up to 20 m/s, however for this study, only velocities up to 10 m/s were used. A function generator provided external inputs to the motor controller for the dynamic inflow velocity variation. For the unsteady cases, phase-locked data was captured using the PIV system, as discussed in section III.D, and ensemble averaged at each phase angle to determine the sensor response to unsteady inflow.

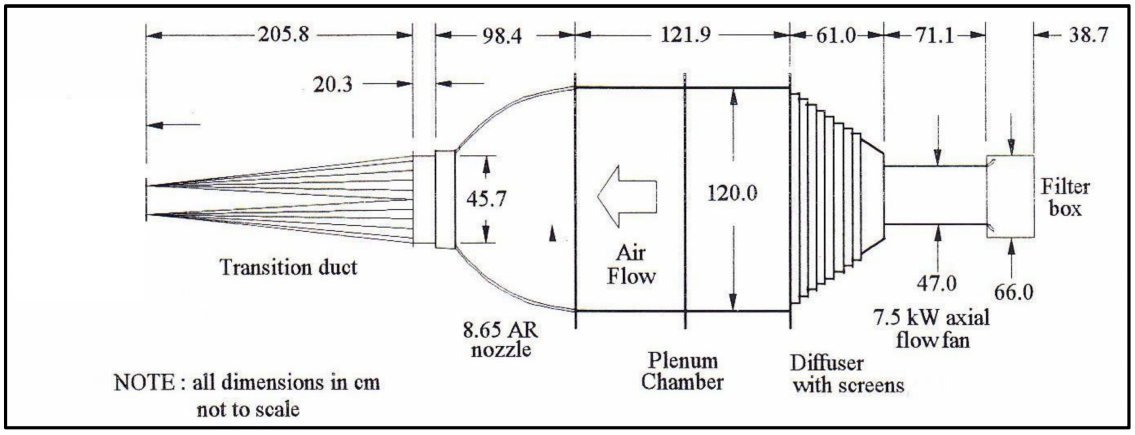

Fig. 2 Schematic of the open-jet wind tunnel circuit used for static and dynamic testing [8].

C. Fluorescent Oil Film Method

The fluorescent oil film method is a flow visualization method, originally developed by Loving and Katzoff [9] at NASA Langley, and modified by Maughmer and Coder [10] at the Pennsylvania State University. The modified version of the oil film method was used as a validation method in static experiments. The method consists of painting a thin layer of oil onto the surface of the NACA 0012. The oil mixture is a 3:1 ratio of AeroShell 100W aviation oil, which fluoresces, to a low-viscosity carrier oil, which thins the mixture. The oil film is painted on the airfoil using a foam paint brush and illuminated by an overhead UV light, which creates high visual contrast in the oil film. The response of the oil film to wind speed is representative of the wall shear at the airfoil surface. Steady state coalescence of the oil film into distinct patterns highlight structures indicative of flow separation and reattachment, which are compared against hot-film sensor data to generate flow separation detection criteria. Because the fluorescent oil film method requires a steady state condition at the airfoil surface, this method of validation is only suitable for static tests.

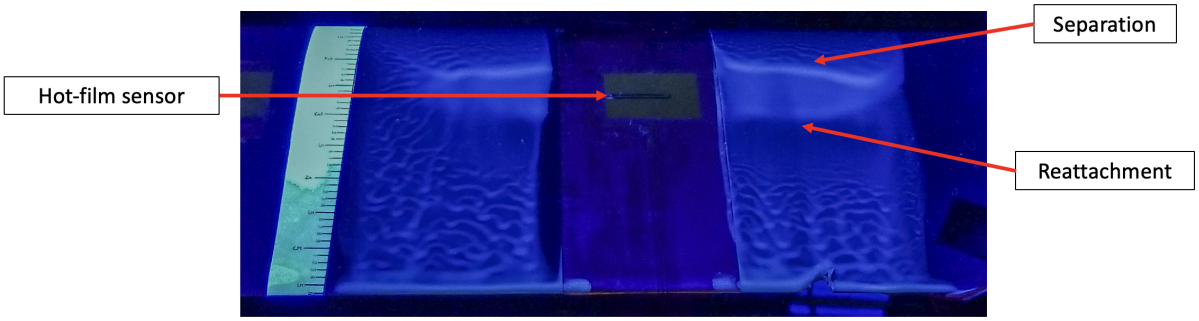

Fig. 3 Fluorescent oil film method. The single hot-film and substrate are shown.

D. Particle Image Velocimetry

Particle image velocimetry (PIV) was the primary validation method used to verify hot-film array performance under unsteady inflow. The PIV system consists of a Quantel Evergreen2 200 mJ 532 nm dual-pulse laser, an Imager sCMOS camera, a LaVision Programmable Timing Unit (PTU-X), and a system PC running the LaVision DaVis imaging software. Aerosolized glycerol serves as the tracer particle and is generated using a fog machine placed directly in front of the filter box at the wind tunnel inlet. Velocity fields are captured by imaging a chordwise wall-normal laser sheet which is projected over the hot-film sensor array. Image acquisition timing is either set in software using the timing box or externally triggered using a TTL signal. For phase-locked data acquisition, the image trigger is provided by the external function generator and phase-locked to the periodic input to the motor controller. Preventive measures are taken to reduce laser reflections, which can harm the quality of the final vector field. No surface treatments were applied directly to the combined hot-film and copper substrate, which was found to be highly reflective and close to

Fig. 4 Linear array hot-film attached to the NACA 0012. The substrate is conformed around the leading and trailing edges of the airfoil. Sensor leads are concealed on the opposite surface of the airfoil extending away from the array to the root and are connected to driving circuitry. A matte black surface treatment is applied to the area surrounding the array to reduce reflections during particle image velocimetry.

the best-performing mirror finish tested by Paterna et al. [11]. The reflective surface of the copper substrate produced superior vector resolution near the surface compared to a matte black finish. A matte black surface finish was still used to treat the areas surrounding the array hot-film to reduce any stray secondary reflections. The hot-film array applied to the airfoil model is shown in figure 4

IV. Results

A. Static Response

Static testing, validated with fluorescent oil film, was first conducted to define a baseline for hot-film sensor response to changing boundary layer condition (attached versus separated). A single hot-film sensor and substrate were primarily used in static testing for simplicity, with wind speed and airfoil angle of attack as free variables to induce a range of separation locations on the airfoil surface. The results of the oil film measurements are shown in Fig. 5a. With this method, separation was detected near the leading edge of the airfoil despite careful preparation of the model. This is likely due to the relatively low Reynolds numbers tested of $Re = 100,000$. For all tested angles of attack, the sensor was located inside the separated zone. Reattachment of the flow was observed at higher angles of attack due to the action of turbulent mixing injecting additional momentum into the near-wall region. Detection of separation via the hot-film occurred by observing the circuit output voltage of the CTA. Contrary to other works using hot-films, it was elected to use the signal variance to detect the separation condition. The sensitivity of the CTA to temperature changes means that this sensor may be subject to significant mean voltage changes in the field, but by quantifying the fluctuations about the mean a more robust method of stall detection can be pursued. Fig. 5 shows the signal variance (obtained by integrating the voltage power spectrum in the frequency domain) to produce the variance over a low-frequency band of 1 Hz to 1 kHz. The sensor detects separation approximately 1 degree after it is indicated by the oil film method. Interestingly this corresponds to a decrease in the signal variance. Following this, near 5 degrees angle of attack the sensor signal reverses and instead records increased variance up to a peak near $\alpha = 9°$. The variance continues to decrease until the oil-film-indicated reattachment zone at approximately 11 degrees α. Establishing a single threshold on the variance for separation detection is challenging due to this observed behavior, however the oil film method only gives limited information into the near-wall flow condition. The initial separation region may come with a reduction in the fluctuating heat transfer level since this is primarily a laminar separation event (at the low Re tested). The reattachment process relies on increased turbulent mixing, which the sensor can detect before reattachment is directly indicated by the oil film. For these reasons, a secondary verification method was pursued using PIV in order to gather additional comparison information on the status of the near-wall flow so that the hot-film sensor behavior could be more clearly interpreted.

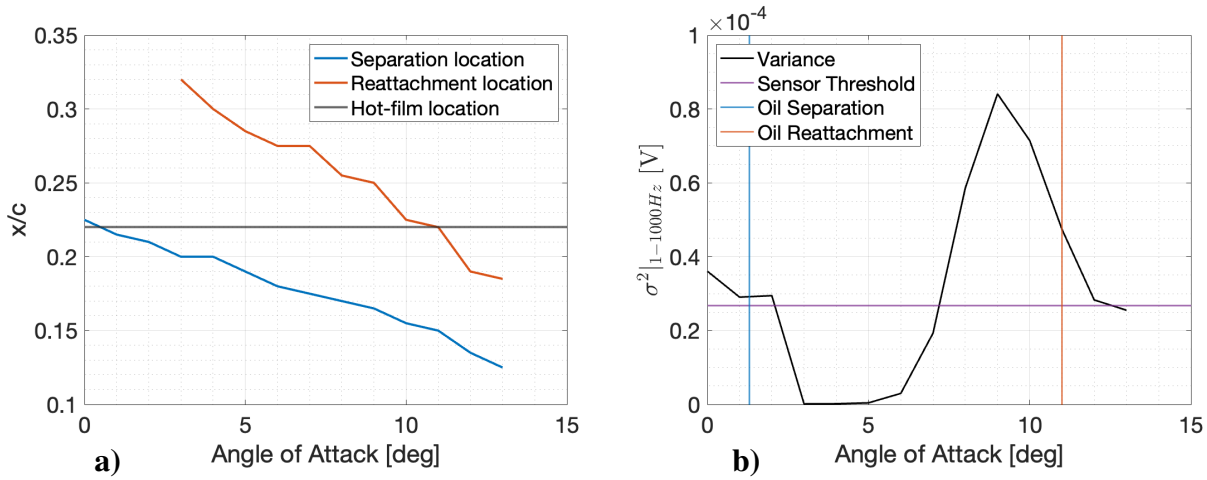

Fig. 5 The separation location and reattachment location interpreted from the oil-film flow visualization is shown in a) along with the location of the single hot-film element at $x/c = 0.22$. The hot-film signal output variance over a 1-1000 Hz band is shown as a black line in b). Also indicated in b) is the separation and reattachment points from the oil film along with the sensor threshold value for separation detection.

B. Unsteady Response

Unsteady testing consisted primarily of gust-response simulation, where the wind tunnel velocity was increased and then decreased in time to obtain different aerodynamic conditions over the linear hot-film array. There were three sensors in the linear hot-film array, one near the leading edge, one at the mid-chord, and one near the trailing edge, as shown in Fig. 4. Wind tunnel velocity variation ranged from 0 to 10 m/s depending on the corresponding gusting frequency, which was limited to 0.25 Hz to accommodate the ramping capability of the wind tunnel fan. The NACA 0012 airfoil model is kept at a constant angle of attack during a gust simulation, with two discreet α values currently being explored: $\alpha = 0°$ and $6°$. These operating points were chosen due to observed movement in the separation and reattachment locations during static testing.

PIV processed ensemble averaged vector fields of the gust simulations show that various periodic unsteady aerodynamic conditions can be produced, including wide regions of turbulent flow and separation bubbles, as seen in figure 6. The ensemble averaged PIV data also confirms the flow condition over any hot-film in the array for different phase angles during the gust simulation. The PIV flow-field data is compared to the time response data taken by the hot-film array and then synchronized in a phase-locked manner, which produces information on the hot-film detection sensitivity to external flow events.

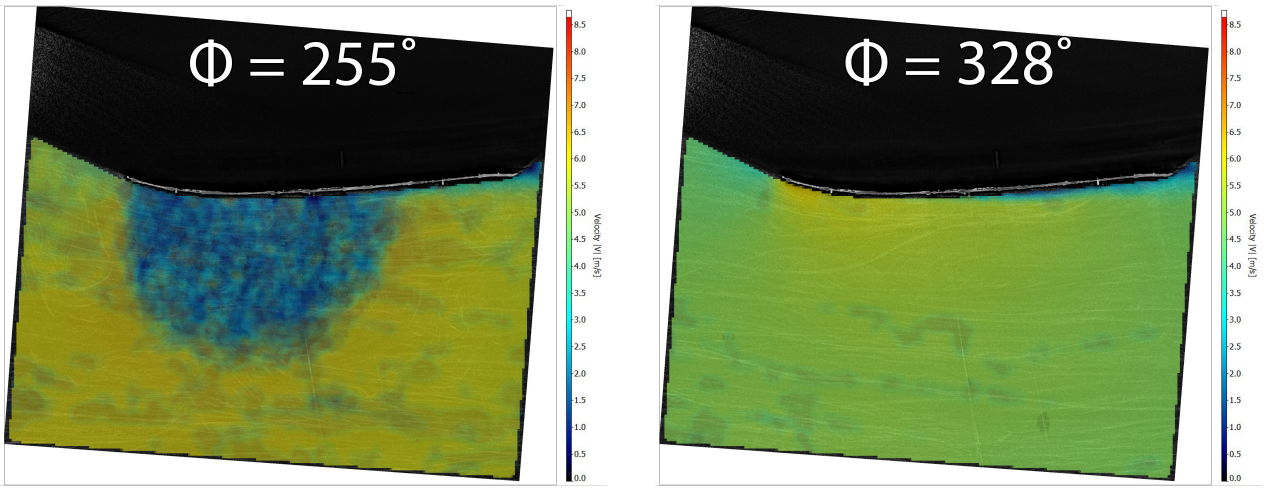

Fig. 6 Gusting velocity variation at different phase angles can produce an unsteady separated region as shown. The velocity contours are ensemble averaged and overlaid onto the raw image acquired by the PIV system to illustrate location relative to the airfoil surface.

Analysis of the ensemble averaged PIV data near the separation location and in regions of separated flow confirm the sensor response observed in static testing, namely that a decrease in the variance corresponds to steady separated flow. Averaged hot-film variance data over the phases of the gusting inflow show that turbulent and recirculating regions of flow actually result in higher integrated variances than that of steady attached flow which can be seen in Fig. 7. This figure shows two cases with differing commanded wind tunnel velocities and two different angles of attack. The commanded wind tunnel velocity is plotted along with the actual velocity measured by the pitot tube as well as the signal variance of the hot-film averaged over multiple cycles of velocity variation. The local minima in the measured pitot tube velocity corresponds to the wind tunnel ramp-down which was intended to cause turbulent flow, such as the unsteady separated region seen in figure 6. This unsteadiness is reflected as an increase in the hot-film variance value. The increase in variance supports the static testing hypothesis that the sensor is actually detecting turbulent fluctuations which are not visualized by the oil-film testing. The ambiguity in sensor variance increase between regular attached flow and turbulent flow means that an overarching lower variance threshold can no longer capture cases of unsteady or transitory separation regions, however the higher integrated variances lend themselves to defining a distinct region of flow which can instead describe pseudo-separated flow or unsteadiness due to the turbulent inflow. The specific behavior of pseudo-separated flow can be described as the airfoil boundary layer sometimes appearing attached or separated. Ensemble averaged PIV smooths out this unsteadiness, which shows up as a larger, low-velocity region as shown in Fig. 6.

A basic method of separation detection is developed which defines regions of separated, attached, and pseudo-separated or unsteady flow based upon an in-situ variance measurement of a known attached flow case. Calibration of the hot-film sensor to a steady attached flow generates a variance baseline which can be used to define two separate, relative thresholds, one for pseudo-separated and another for steady separated flow, the latter of which has low to no observed intermittency. In general, the ensemble averaged PIV data can be used to determine if the flow is attached or in a separated/turbulent condition. However, the limited resolution of PIV for velocities close to the airfoil surface means the difference between pseudo-separated or unsteady attached flow is sometimes unresolvable. In the case of separated flow, data from the trailing edge hot-film sensor in the array is used as a reference to define a threshold for steady separated flow, as the trailing edge sensor operated almost completely in the region of separated flow during experiments. Based upon measurements for the trailing edge sensor, it was found that steady separated flows have integrated variance at least two orders of magnitude lower than that of an attached flow. The variances measured by trailing edge hot-film for steady separated flow are on the order of 10^{-7}. The leading edge hot-film produces variances on the order of 10^{-4} as seen in Fig. 8 and Fig. 5 in attached and pseudo-separated cases. Statically, the single hot-film sensor was able to demonstrate steady separated behavior in angles of attack of 3° to 5°. The flow condition of the leading edge hot-film in the array never reaches a steady separated state due to the parameters of the experiment, which can be seen in figure 8. For pseudo-separated or turbulent regions, an empirically determined factor of 1.25 times the fully attached baseline flow was found to be a good threshold for differentiating pseudo-separated, turbulent, or

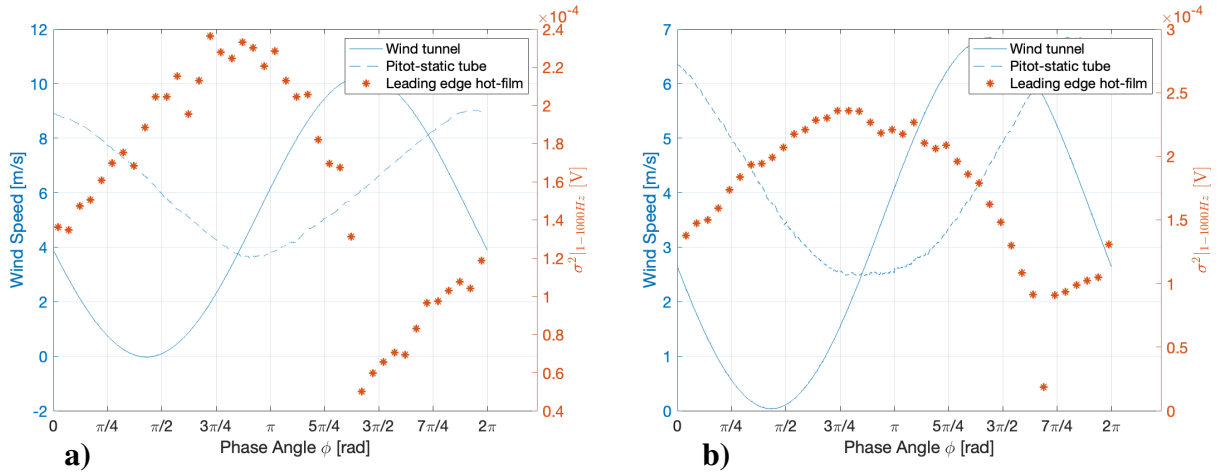

Fig. 7 Wind tunnel input, pitot-static tube, and hot-film variance data are plotted over a period of sinusoidal unsteady input where a) shows an α = 0° case and b) shows an α = 6° case. Velocities are associated with the left-most ordinates while the hot-film data is shown on the right ordinates. Pure separation was intended at the minimum wind speed output, however, the hot-film sensor response indicates unsteadiness and turbulence in the near-wall flow. This state is classified as pseudo-separated due to the intermittency between attached and separated conditions.

transitory separation flow from attached flow, at least for the *Re* range tested. These baselines and thresholds are plotted for 0° and 6° angle of attack cases in figure 8 for the same two distinct cases of inflow as figure 7. In figure 8 the variance values from both hot-films are shown over the entire period of gust variation. The baseline variance values can be seen, which are only using to define the relative thresholds for pseudo-separated flow and steady separated flow. In figures 8a and 8b, separate baselines were selected based on the phase angle using an observed steady attached flow as a reference for each case. The 1.25 factor multiplying the baseline can be seen to capture the entirety of the region of pseudo-separated flow, found using PIV. The factor multiplying the baseline is not constant and can change depending on *Re* as it depends on the turbulent kinetic energy present in the freestream as well as whether the boundary layer is laminar or turbulent prior to separation.

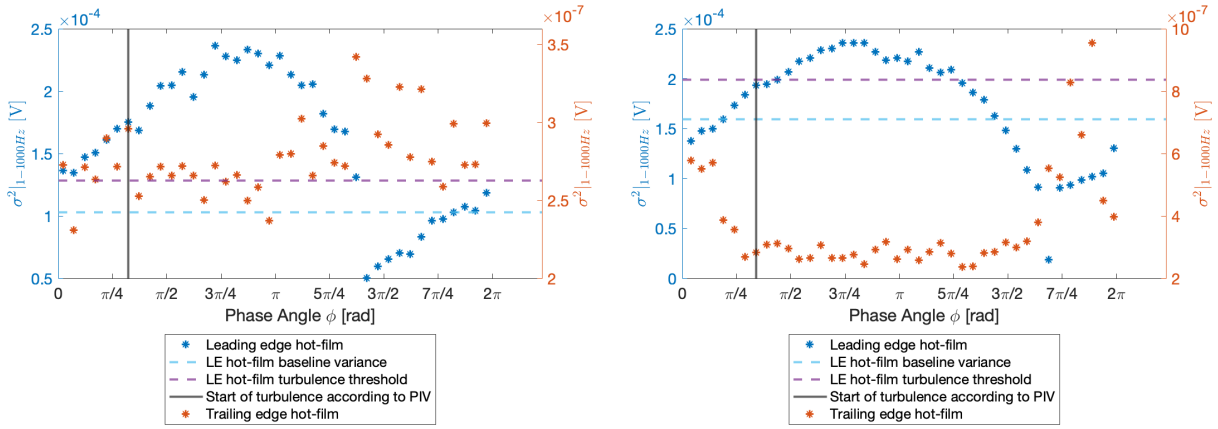

Fig. 8 The baseline and turbulent threshold variances are defined for the leading edge hot-film as shown in the figure in a) for $\alpha = 0°$ and in b) for $\alpha = 6°$. Leading edge hot-film data is associated with the left ordinate while the trailing edge is shown on the right ordinate for each plot. Above the turbulence threshold (shown by the purple line), the flow can be assumed to be pseudo-separated. The threshold conservatively predicts separation compared to validation data taken with PIV. Variance data is shown for the trailing edge hot-film, which serves as the reference for steady separated flow.

V. Conclusions

A process for fabrication and simple method of separation detection is presented for a large-array hot-film. Fabrication is outlined from raw materials to the final working sensor array. Detection of separated flow is possible through variance integrated in the frequency domain, which serves as a robust indicator of the flow state when calibrated to a reference variance. The results highlight the necessary steps for future development of the hot-film array, which include finding a low-cost alternative to the research grade CTA and continued testing at scaled Reynolds numbers to assess viability of the threshold to detect separated flow in the field.

Acknowledgments

References

[1] Schreivogel, P., and der TU Dresden eV, A. F., "Detection of laminar-turbulent transition in a free-flight experiment using thermography and hot-film anemometry," *27th Congress of International Council of the Aeronautical Sciences*, 2010.

[2] Poggie, J., Tilmann, C. P., Flick, P. M., Silkey, J. S., Osbourne, B. A., Ervin, G., Maric, D., Mangalam, S., and Mangalam, A., "Closed-loop stall control system," *Journal of Aircraft*, Vol. 47, No. 5, 2010, pp. 1747–1755.

[3] Sturm, H., Dumstorff, G., Busche, P., Westermann, D., and Lang, W., "Boundary layer separation and reattachment detection on airfoils by thermal flow sensors," *Sensors*, Vol. 12, No. 11, 2012, pp. 14292–14306.

[4] Lee, T., and Basu, S., "Measurement of unsteady boundary layer developed on an oscillating airfoil using multiple hot-film sensors," *Experiments in Fluids*, Vol. 25, No. 2, 1998, pp. 108–117.

[5] Shikida, M., Yoshikawa, K., Iwai, S., and Sato, K., "Flexible flow sensor for large-scale air-conditioning network systems," *Sensors and Actuators A: Physical*, Vol. 188, 2012, pp. 2–8.

[6] Menegozzo, L., Dal Monte, A., Benini, E., and Benato, A., "Small wind turbines: A numerical study for aerodynamic performance assessment under gust conditions," *Renewable energy*, Vol. 121, 2018, pp. 123–132.

[7] Onol, A. O., and Yesilyurt, S., "Effects of wind gusts on a vertical axis wind turbine with high solidity," *Journal of Wind Engineering and Industrial Aerodynamics*, Vol. 162, 2017, pp. 1–11.

[8] Town, J., and Camci, C., "Sub-miniature five-hole probe calibration using a time efficient pitch and yaw mechanism and accuracy improvements," *Turbo Expo: Power for Land, Sea, and Air*, Vol. 54631, 2011, pp. 349–359.

[9] Loving, D. L., and Katzoff, S., "The Fluorescent-Oil Film Method and Other Techniques for Boundary-Layer Flow Visualization," Tech. rep., 1959.

[10] Maughmer, M. D., and Coder, J. G., "Comparisons of theoretical methods for predicting airfoil aerodynamic characteristics," Tech. rep., AIRFOILS INC PORT MATILDA PA, 2010.

[11] Paterna, E., Moonen, P., Dorer, V., and Carmeliet, J., "Mitigation of surface reflection in PIV measurements," *Measurement science and technology*, Vol. 24, No. 5, 2013, p. 057003.